Geoderma 169 (2011) 47–54

Contents lists available at ScienceDirect

Geoderma

journal homepage: www.elsevier.com/locate/geoderma

Wettability of kaolinite (001) surfaces — Molecular dynamic study

Roland Šolc [a,*], Martin H. Gerzabek [a], Hans Lischka [b], Daniel Tunega [a,b,**]

[a] Institute of Soil Research, University of Natural Resources and Life Sciences, Vienna, Peter-Jordan-Strasse 82, A-1190 Vienna, Austria
[b] Institute for Theoretical Chemistry, University of Vienna, Währinger-Strasse 17, A-1090 Vienna, Austria

ARTICLE INFO

Article history:
Received 15 June 2010
Received in revised form 3 January 2011
Accepted 8 February 2011
Available online 25 March 2011

Keywords:
Kaolinite
Contact angle
Molecular dynamics

ABSTRACT

Wettability of two (001) basal kaolinite surfaces (tetrahedral and octahedral) was investigated by means of force-field molecular dynamics simulation. Water nanodroplets were deposited on the surfaces and microscopic contact angle was determined from a droplet profile. In case of the octahedral surface the nanodroplet was spread on the surface forming an incomplete monomolecular layer. Multiple, relatively strong hydrogen bonds of the water layer with the surface hydroxyl groups are responsible for the spreading. The contact angle for the octahedral surface is equal zero, thus this surface is strongly hydrophilic. In case of the tetrahedral surface water molecules of the droplet stayed together forming a deformed sphere on the surface. The computed microscopic contact angle is about 105° meaning that the tetrahedral surface is hydrophobic. In spite of weak interactions of the droplet with this surface the water in the vicinity of the surface is structured and ordered into a form of monomolecular water layers with altering density what reflects a polarization effect of the surface. The experimental values of contact angle for kaolinite are about 20° which indicates that the overall character of the kaolinite surface is hydrophilic and our calculations document that a key factor for this property is surface hydroxyl groups of the octahedral surface.

1. Introduction

Clay minerals form a major part of inorganic matter of soils and have a significant impact on physicochemical processes in soils. They contribute to processes such as driving transport, distribution, stability, and retention of dissolved organic/inorganic species in soil solutions (Rae and Parker, 1988; Schachtschabel et al., 1989). Clays are often used in various chemical, medical, geological, material, and related industrial applications (Bailey, 1988). Natural clays predominantly exist in a form of small particles (few μm in diameter or less) what predetermines their high specific surface area and high chemical surface activity. These characteristics can be directly related to physicochemical properties of clays such as swelling, wetting, adsorption, ion-exchange, reactivity, catalytic activity, etc. A specific feature is the capability of a number of clays to accommodate various molecular species in their interlayer spaces. In many of related processes, a significant role plays contact of mineral surface with solution or pure liquid water since water is a natural solvent and transport medium for chemical species. Thus, a detailed understanding of clay–water interfaces is in a center of interest. Molecular modeling techniques are extensively used in a study of these interfaces and numerous papers can be found in literature.

Among rich group of natural clay minerals, kaolinite ($Al_2Si_2O_5(OH)_4$) has an important role because of its high abundance in nature, relatively pure chemical composition, and well characterized crystal structure (Adams, 1983; Bish, 1993; Neder et al., 1999; Young and Hewat, 1988). Owing to layered structure kaolinite microparticles exist in a form of hexagonal plates (Vaz et al., 2002) with dominant, almost perfectly cleavaged (001) basal surfaces. Kaolinite is a di-octahedral layered aluminosilicate of 1:1 type, therefore, each layer has two different surfaces parallel to the (001) plane. First one, tetrahedral, is formed from basal oxygen atoms of the tetrahedral (SiO_4) sheet, while second one, octahedral, is formed from surface hydroxyl groups of the octahedral (AlO_6) sheet (Fig. 1).

The structure and active sites of both (001) basal surfaces and their interactions with water have been intensively studied by various molecular modeling methods. A thin water layer of several Å thickness confined between two kaolinite layers has been simulated by means of classical molecular dynamics (MD) using empirical force-field (FF) parameters for interatomic interactions (Smirnov and Bougeard, 1999). In that work a different structural orientation of water molecules at both surfaces was observed. In another FF-MD study, extended interlayer spacing of several tens of Å filled with water was modeled (Warne et al., 2000). It was found that water molecules at the hydroxylated surface show a marked decrease in the self-diffusion coefficient and an increase in the rotational correlation time. Simulation of water adsorption and ice nucleation on both (001)

* Corresponding author. Tel.: +43 1 47654 3131; fax: +43 1 47654 3130.
** Correspondence to: D. Tunega, Institute for Theoretical Chemistry, University of Vienna, Währinger-Strasse 17, A-1090 Vienna, Austria.
E-mail addresses: roland.solc@boku.ac.at (R. Šolc), daniel.tunega@boku.ac.at (D. Tunega).

0016-7061/$ – see front matter © 2011 Elsevier B.V. All rights reserved.
doi:10.1016/j.geoderma.2011.02.004

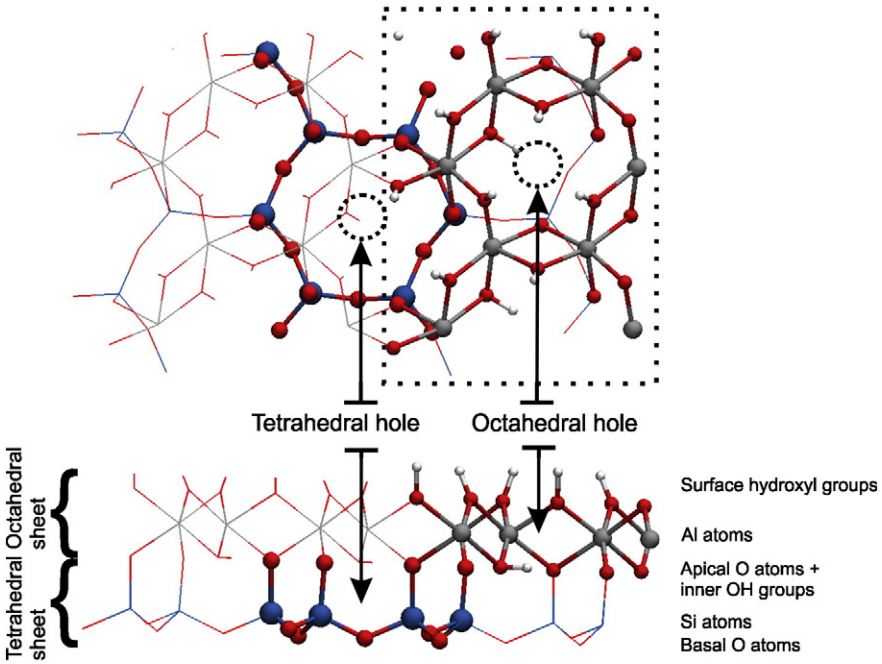

Fig. 1. Structure of kaolinite layer. Top (upper) and side (lower) views.

kaolinite surfaces under atmospheric conditions was performed using a grand canonical Monte Carlo (MC) approach (Croteau et al., 2008, 2009). A significant difference in affinity of water to siloxane and hydroxylated surfaces was observed. Detailed quantum chemical studies (density functional theory based, DFT) including molecular dynamics have been carried out on hydrogen bonding and interactions of isolated water molecule and monomolecular water layer with both (001) kaolinite surfaces (Tunega et al., 2002a, 2002b, 2004). Calculated interaction energies of water showed a large difference between both surfaces. The tetrahedral surface was quantified as hydrophobic while the octahedral surface as hydrophilic. In order to understand a role played by kaolinite in heterogeneous ice nucleation, DFT study was performed for water on its (001) basal plane using a varying amount of water molecules (Hu and Michaelides, 2007, 2008). Strong binding and clustering of water was observed for the octahedral surface.

Theoretical studies have shown that kaolinite has two structurally and chemically different (001) surfaces what, as a consequence, will have a significant impact on overall macroscopic properties of mineral particles such as wettability. Wetting phenomena have long served as a means of characterizing hydrophobic/hydrophilic character of solid surfaces. Experimentally, wettability can be determined e.g. by means of contact angle (CA) measurements. Using CA method surface free energy of solids can also be computed. Determination of the CA for clay minerals is usually difficult because CA measurements are affected by various factors such as temperature, relative humidity, particle shape and size, surface heterogeneity and roughness, etc. (Shang et al., 2010). Therefore, it is practically impossible to distinguish and characterize individual surfaces using the CA method if measured matter is in a form of soft powder with particles of microscopic size. In spite of that there are several experimental studies on wettability of kaolinite. For example, the surface free energy of kaolinite of 252.57 ± 2.75 mJ/m^2 was determined using the CA method (Helmy et al., 2004). The contact angle of $16.9 \pm 0.7°$ was measured for kaolinite at 33% relative humidity indicating that overall kaolinite surface is hydrophilic (Shang et al., 2010). However, none of those experimental studies did not estimate what types of kaolinite surfaces contribute to the measured values. Therefore, in this view, theoretical methods seem to be extremely useful because on the base of knowledge of mineral structure and morphology of particles they allow simulation of particular mineral surface with the full control of computing conditions.

In recent years several molecular simulations were performed in the study of surface properties of solid matter simulating interactions of liquid nanodroplets (mostly water) with various surfaces (Cruz-Chu et al., 2006; Giovambattista et al., 2007; Hong et al., 2009; Ingebrigtsen and Toxvaerd, 2007; Lundgren et al., 2002; Ohler and Langel, 2009; Park and Aluru, 2009; Shi and Dhir, 2009; Werder et al., 2003). These studies typically used either Monte Carlo or molecular dynamics methods applying classical force fields for describing intermolecular interactions. This type of simulation is usually very time demanding because of large simulation models, usually comprising thousands or more atoms. It has been shown that used approach is suitable for modeling of microscopic contact angle and obtained results can be directly comparable to experimental macroscopic observations. For example, MD studies of the contact angle of the water droplet on amorphous silica surface have demonstrated that hydrophilicity of the surface increases with increasing concentration of surface silanol groups (Cruz-Chu et al., 2006). Moreover, in that work the contact angle calculations have been used for the optimization of force field parameters. In another study, MD simulations of the water droplet in the contact with rutile (TiO_2) surfaces have shown that temperature is an important parameter controlling the surface wettability (Park and Aluru, 2009).

In present paper, we investigate wetting properties of both (001) basal kaolinite surfaces, tetrahedral and octahedral, applying molecular dynamics simulations of contact angle for water nanodroplets placed on surfaces. The aim is to characterize and quantify hydrophobic/hydrophilic property of both dominant kaolinite surfaces and explain observed differences.

2. Structural and simulation details

The crystal structure of kaolinite is well-known and has been described many times. Therefore, we only briefly depict our surface models. Kaolinite is typical mineral with a layered structure consisting of aluminosilicate layers of 1:1 type (Fig. 1). Layers are connected in a bulk structure via hydrogen bonds formed between surface hydroxyl groups of the alumina octahedral sheet and basal oxygen atoms of the silica tetrahedral sheet of the adjacent layer. In our study we used a model of isolated kaolinite layer possessing both (001) basal surfaces,

tetrahedral terminated with a plane of basal oxygen atoms, and octahedral terminated with a plane of surface hydroxyl groups, respectively (Fig. 1). The atomic positions in the layer model were taken from the experimental crystal structure of kaolinite derived in low-temperature neutron powder diffraction experiment (Bish, 1993). The crystal structure was determined as a triclinic possessing $C1$ symmetry with parameters $a = 5.1535$ Å, $b = 8.9419$ Å, $c = 7.3906$ Å, and $\alpha = 91.926°$, $\beta = 105.046°$, $\gamma = 89.797°$.

Since in our simulations only isolated kaolinite layer was modeled, a rectangular shape of computational cells was used. The size of each cell was derived by multiplication of experimental a, b, and c vectors. Suitability of used force fields was verified by the calculation of interaction energy between surface of the kaolinite layer and single water molecule using computational cell of $30.921 \times 35.7676 \times 110.859$ Å. In the case of CA calculations the cell size was depended on the size of the water nanodroplet. The first model consisted of the water droplet containing 100 water molecules ($N_w = 100$) and the clay layer situated in a simulation cell of $82.456 \times 80.477 \times 110.859$ Å. The second model was represented by the kaolinite layer and the droplet containing 500 water molecules with a cell size of $123.684 \times$ v 125.187×177.375 Å. The third model was constructed from the water droplet with 1000 molecules deposited on kaolinite surface(s) in a computational box of $144.298 \times 143.071 \times 192.156$ Å. In all cases the periodic boundary conditions were applied in all directions. The water nanodroplets before their localization above the kaolinite surfaces were equilibrated in a short MD run of 1 ns length. After that droplets were positioned in the middle of the computational cell at a distance of ~3 Å from the kaolinite surface to the bottom border of the droplet. Figs. 2a and 3a display an initial configuration of the water nanodroplet containing 500 molecules placed above the octahedral and/or tetrahedral surface, respectively.

All MD calculations were performed using LAMMPS simulation package (Plimpton, 1995). The kaolinite layer was described by means of CLAYFF force field (Cygan et al., 2004). The CLAYFF field was developed for a study of hydrated crystalline compounds and their interfaces with fluid phases and is represented by a short range Lennard-Jones (LJ) part, and a long range Coulombic part expressed in a form of pairwise interacting atomic charges. Thus, total interaction energy is given by the sum of Coulombic and LJ terms:

$$E_{\text{total}} = E_{\text{Coul}} + E_{\text{LJ}} = \frac{e^2}{4\pi\varepsilon_0}\sum_{i\neq j}\frac{q_i q_j}{r_{ij}} + 4\varepsilon_{ij}\sum_{i\neq j}\left[\left(\frac{\sigma_{ij}}{r_{ij}}\right)^{12} - \left(\frac{\sigma_{ij}}{r_{ij}}\right)^{6}\right] \quad (1)$$

where in the Coulombic term, q_i and $q_{j,}$ are partial atomic charges, r_{ij} is a distance between atoms i and j, e is the charge of electron, and ε_0 is dielectric permittivity of vacuum. Van der Waals energy term (E_{LJ}) is defined by a conventional $(12-6)$ function, where r_{ij} is distance between atoms i and j, σ_{ij} is distance at which interaction energy of two atoms is minimal, and ε_{ij} is characteristic energy. The van der Waals interaction between different atomic species i and j are calculated using arithmetic combination rule:

$$\varepsilon_{ij} = \sqrt{\varepsilon_i \varepsilon_j}; \quad \sigma_{ij} = \left(\sigma_i + \sigma_j\right)/2. \quad (2)$$

Nonbonding CLAYFF parameters of all atom types of the kaolinite layer used in this work are collected in Table 1. During the simulations the positions of all atoms of the kaolinite layer were fixed except the surface OH groups what required a bonding field to describe them. For this purpose the same harmonic stretching parameters as for SPC (SPC/E) water (see later) were used (Table 2).

In a description of water molecule, three force-filed models were used – two point charge models SPC and SPC/E (Berendsen et al., 1981, 1987; Kusalik and Svishchev, 1994), and TIP4P model (Jorgensen and Madura, 1985). In fact, the SPC/E model is reparametrized SPC with slightly modified atomic charges (Table 1). The SPC model was included in calculations because the CLAYFF model was originally parameterized to be a consistent with this water force field. In all simulations the water molecules were kept rigid using the SHAKE algorithm (Ryckaert et al., 1977). Nonbonding and bonding parameters of all three water models are collected in Tables 1 and 2. Intermolecular interactions between atoms of the kaolinite layer and water molecules were expressed by means of CLAYFF parameters.

In molecular dynamics, the Newton's equations of motion were numerically integrated using the Verlet velocity algorithm (Swope et al., 1982) with a time step of 1.0 fs. For calculation of CA the van der Waals interactions were truncated using a 12 Å cutoff. Coulombic electrostatic interactions were computed using the Ewald method (Ewald, 1921) for water droplets described by the SPC and SPC/E models, respectively, and using the Particle–Particle Particle-Mesh (PPPM) method (Hockney and Eastwood, 1988) for the TIP4P model. Cutoff for Coulombic interactions was always half of the shortest cell vector of the computational cell avoiding long range interactions between water droplets in neighboring cells. All CA simulations were performed using canonical (NVT) ensemble at temperature $T = 300$ K what was controlled by rescaling atomic velocities during the MD run.

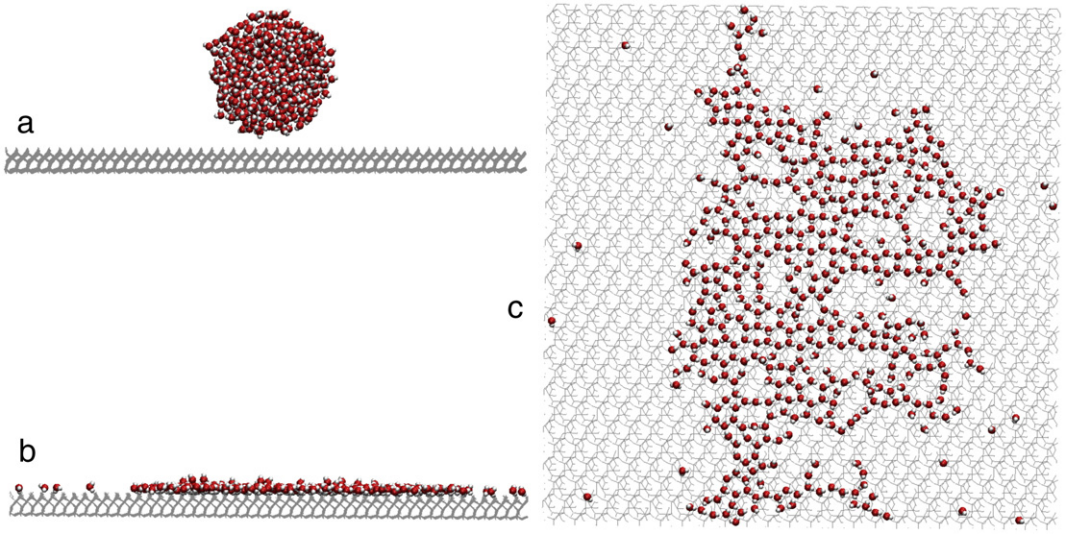

Fig. 2. Snapshots from MD for SPC/E water droplet with $N_w = 500$ placed on the (001) octahedral surface of the kaolinite layer: initial geometry (a), front (b) and top (c) view after 5 ns.

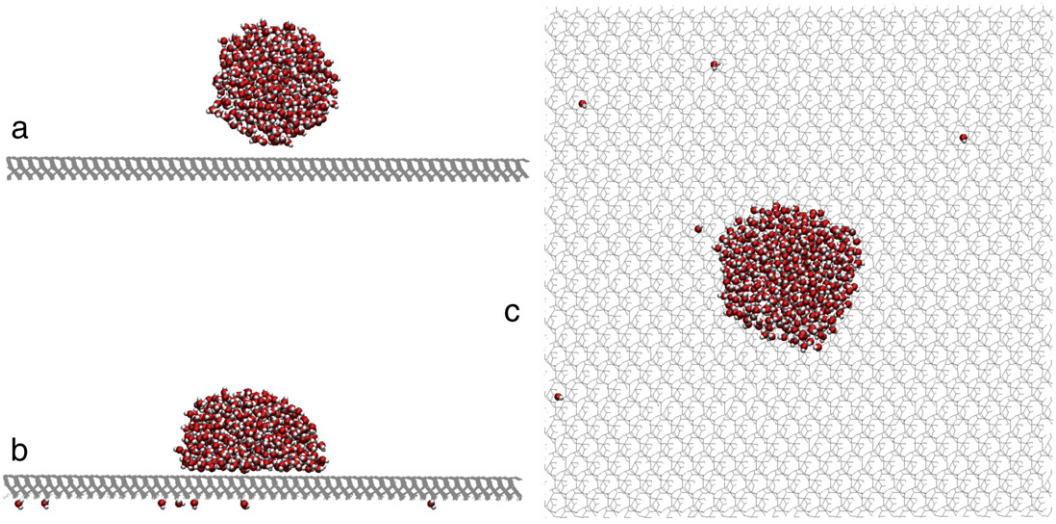

Fig. 3. Snapshots from MD for SPC/E water droplet with $N_w = 500$ placed on the (001) tetrahedral surface of the kaolinite layer: initial geometry (a), front (b) and top (c) view after 5 ns.

The total simulation lengths were 10 ns for $N_w = 100$, 5 ns for $N_w = 500$, and 3 ns for $N_w = 1000$, respectively. In analysis, last 2 ns was used, the rest of the MD run was considered as an equilibration phase.

Suitability of the used force fields (SPC, SPC/E and TIP4P) was checked by means of the *NVT* MD of the single water molecule interacting with both kaolinite surfaces at 10 K. The interaction energy was calculated as a difference between averaged potential energy of the water-layer model and the sum of the averaged potential energies of the isolated water molecule and the isolated kaolinite layer, respectively. The averaged potential energies were calculated from last 25 ps of 100 ps MD run, always using the same MD conditions.

2.1. Contact angle

Wettability of surface is usually expressed in terms of contact angle measurement. If the CA between liquid and solid surface is less than 90°, the surface is called hydrophilic, otherwise the surface is called hydrophobic. If the CA of water droplet on hydrophilic surface is in a range of 0-30° this surface is called superhydrophilic. In case of superhydrophobic surfaces the CA exceeds 150° that means that these surfaces are extremely difficult to wet.

In our simulations a microscopic contact angle was computed from a fit of circle equation to contour of water droplet as is shown in Fig. 4. For this purpose it was necessary to determine a droplet boundary using a method of cylindrical bins for mapping water density in the droplet (de Ruijter et al., 1999). The *xy*-plane is defined as the plane parallel to the (001) basal surface of the kaolinite layer while the *z*-axis is defined as the axis passing through the center of mass of the droplet perpendicular to the *xy*-plane. Water droplet on the surface posses an azimuthal symmetry, thus usage of (*R*,*z*) coordinate system is useful. Directions *R* and *z* are discretized onto cylindrical bins using steps of $\Delta R \approx 0.8$–1.0 Å and $\Delta z \approx 0.2$–0.3 Å, respectively. For each cylindrical bin averaged density of water is calculated and the droplet boundary is considered if the water density is half of the bulk water density (0.5 g/cm^3). To find a particular point of the droplet boundary for each *z* slab following tanh function describing water density relation at liquid–gas interface has been used:

$$\rho(R) = \frac{\rho_1}{2}\left(1 - \tanh\left(\frac{2(R-R_e)}{w}\right)\right). \quad (3)$$

In this equation is assumed that the vapor density is zero, ρ_1 is the density inside of the droplet, *R* is the distance from origin to the droplet surface, R_e is the center of interface region (meaning a boundary point) and the thickness of the interface is given by *w*. The particular water density points in one of the first *z*-slabs for droplet with $N_w = 500$ (SPC/E) and corresponding fit curve are shown in Fig. 5. The fitting parameters for this particular fit are $\rho_1/2 = 0.551 \pm 0.003$ g/cm^3, $R_e = 17.29 \pm 0.05$ Å, and $w = 3.58 \pm 0.17$ Å, and *rms* = 0.008. The obtained set of R_e points has been used in a least-squares circle fitting method and resulting fitting curve is indicated by a thin line in Fig. 4. The computed contour curve was then

Table 1
Nonbonding parameters of the CLAYFF force field (Cygan et al., 2004) and of three water models (Berendsen et al., 1987; Jorgensen and Madura, 1985; Kusalik and Svishchev, 1994).

Species	Symbol	Charge (*e*)	ε_0 (kcal/mol)	σ_0 (Å)
Octahedral aluminum	ao	1.5750	1.3298E-06	4.2713
Tetrahedra silicon	st	2.1000	1.8405E-06	3.3020
Bridging oxygen	ob	−1.0500	0.1554	3.1655
Hydroxyl oxygen	ho	−0.9500	0.1554	3.1655
Hydroxyl hydrogen	oh	0.4250		
SPC water oxygen	o_w	−0.82	0.1553	3.1660
SPC water hydrogen	h_w	0.41		
SPC/E water oxygen	ospc	−0.8476	0.1553	3.1660
SPC/E water hydrogen	hspc	0.4238		
TIP4P water oxygen	otip	−1.0484	0.1628	3.1644
TIP4P water hydrogen	htip	0.5242		

Table 2
Bond stretch and angle bend parameters of harmonic potential for the surface OH group and water molecule. K_1 represents force constant and r_1 and r_2 are equilibrium bond distances, respectively. K_2 represents force constants and Θ_0, φ_0 are equilibrium angles.

Bond stretch				
Species *i*	Species *j*	K_1 (kcal/mol Å^2)	r_1 (Å)	r_2 (Å)
oh	ho	554.1349	1.0000	
o_w	h_w	554.1349	1.0000	
ospc	hspc	554.1349	1.0000	
otip	htip	554.1349	0.9572	0.1500

Angle bend					
Species *i*	Species *j*	Species *k*	K_2 (kcal/mol rad^2)	Θ_0 (deg)	φ_0 (deg)
h_w	o_w	h_w	45.7696	109.47	
hspc	ospc	hspc	45.7696	109.47	
htip	otip	htip	45.7696	104.52	52.26

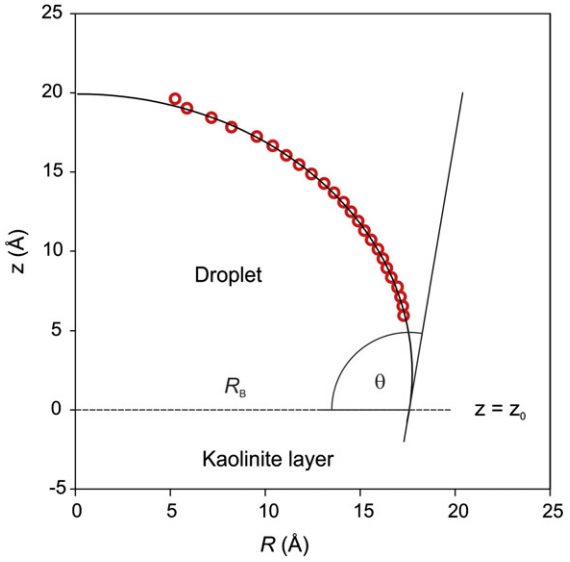

Fig. 4. Schematic for computation of water liquid–gas boundary and contact angle θ, z_0 is the z-position of the top/most tetrahedral kaolinite layer (plane of basal oxygen atoms), and R_B represents radius of fitted circle. The contact angle is measured in a point where kaolinite surface (dashed line) crosses fitted circle.

extrapolated and at the crossing point with the dashed line representing the surface of kaolinite the contact angle θ was measured (Fig. 4).

3. Results and discussion

3.1. MD simulation of single water molecule

In the first part of the work, suitability of the CLAYFF force field for interactions of water molecules with kaolinite was tested by performing 10 K MD simulations on models of the single water molecule (SPC, SPC/E and TIP4P) interacting with both kaolinite surfaces. Calculated interaction energies are collected in Table 3 and are compared to the results obtained by FF Monte Carlo simulations (SPC/E water model) at 10 K (Croteau et al., 2009), and by DFT methods (Tunega et al., 2002a, 2002b), respectively. Details to MC and both DFT calculations can be found in the cited references. Our all three MD simulations showed that the surface OH groups of the octahedral surface are flexible having ability to form multiple hydrogen bonds with polar molecules, where these groups can act as a proton donor or acceptor. Formed surface complex is stable having three hydrogen bonds where two surface hydroxyl groups are proton donors to the water oxygen, and the third OH group is proton acceptor with respect to the water molecule, respectively. Similar complex was observed in MC (Croteau et al., 2009) and DFT studies (Tunega et al., 2002a, 2002b). Calculated interaction energies for all three water FF models are from −13.3 kcal/mol (SPC) to −14.0 kcal/mol (SPC/E and TIP4P) what are values close to energy of −14.7 kcal/mol obtained by the DFT calculations (PW91 functional) on the periodic model (Tunega et al., 2002a), and is in a relatively good agreement with the second theoretical value of −10.5 kcal/mol obtained at the B3LYP/SVP level of the theory and using cluster model (Tunega et al., 2002b). Table 3 shows that FF Monte Carlo calculations (Croteau et al., 2009) have provided interaction energy of −11.1 kcal/mol for the SPC/E water model differing by 2.9 kcal/mol from our SPC/E result.

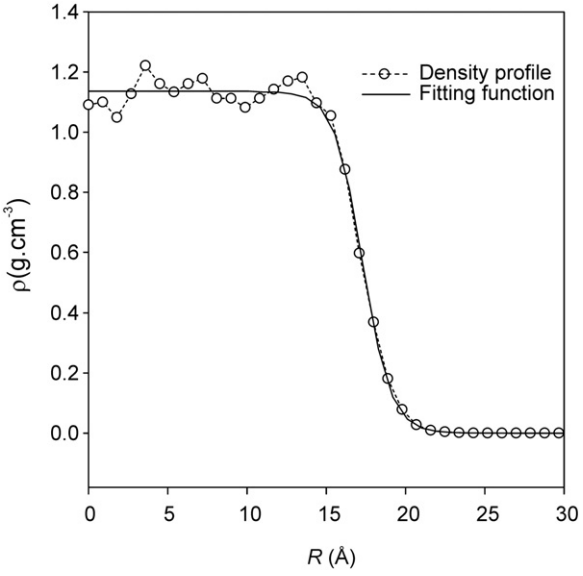

Fig. 5. Water density ρ (in g/cm^3) in one of the first z-slabs of the water droplet as a function of distance R from z-axis (crossing the center of mass of the droplet) obtained for last 2 ns of MD simulation for $N_w = 500$ (SPC/E).

For the tetrahedral surface our MD simulation has shown that the water molecule forms weakly bound surface complex with one not very stable hydrogen bond. Similar complex was also observed in the MC (Croteau et al., 2009) and both DFT simulations, respectively (Tunega et al., 2002a, 2002b). All three calculated interaction energies are about −6 kcal/mol (Table 3) being a little larger than both DFT values (−4.1 and −3.8 kcal/mol, Table 3). The interaction energy of −5.2 kcal/mol obtained in the MC study (SPC/E water model) (Croteau et al., 2009) is in an agreement with our results.

In spite of some small differences between FF MD and MC results it can be concluded that the CLAYFF describes interactions of water molecules with kaolinite surfaces properly showing a clear difference between both surfaces.

3.2. MD simulations of water droplets

3.2.1. Octahedral surface

Fig. 2a shows a front view of the initial configuration of the water droplet with 500 SPC/E molecules placed on the (001) octahedral surface of the kaolinite layer. Fig. 2b and c display front and top side views of a snapshot collected after 5 ns MD run. Observed is a complete spreading of the water droplet on the surface and formation of an incomplete monomolecular water net. Water molecules form two types of hydrogen bonds, among themselves and with the surface hydroxyl groups. The incomplete water layer is relatively good structured having clearly formed quasi-hexagonal rings what evidently reflects positions of the surface hydroxyl groups. This is also in accordance with observed ice-like nucleation of water on the octahedral surface in previous DFT studies (Hu and Michaelides, 2007, 2008). The overall pattern of the water layer is partially floating due to a rearrangement and reordering of hydrogen bonds during MD. This scenario (spilling of water droplet during the MD run) was observed for all models with the octahedral surface ($N_w = 100/500/1000$, SPC/E, TIP4P) and similar pattern of incomplete water layer was always formed.

Of course, in case of the octahedral surface, we cannot calculate contact angle in a way as described above since the compact water

Table 3
Calculated interaction energies, ΔE (kcal/mol), for single water molecule on the octahedral and tetrahedral surface of the kaolinite layer obtained from the static relaxation using CLAYFF (this work), periodic DFT/PW91[a] (Tunega et al., 2002a) and B3LYP/SVP[a] (Tunega et al., 2002b).

Surface	MD SPC	MD SPC/E	MD TIP4P	MC SPC/E	DFT/PW91	B3LYP/SVP
Octahedral	−13.3	−14.0	−14.0	−11.1	−14.7	−10.5
Tetrahedral	−5.9	−6.0	−6.4	−5.2	−4.1	−3.8

[a] For details see original references.

droplet was transformed to the incomplete monomolecular water network. In this situation the contact angle is equal zero and the octahedral surface can be considered as superhydrophilic. To show a general picture of the water molecules distributed on the octahedral surface, one-dimensional atomic density profile of water oxygen atoms was calculated in a direction perpendicular to the kaolinite surface. This density profile is normalized with respect to number of snapshots collected for analysis and the volume of bin in the z-direction. The curves corresponding to 100/500/1000 SPC/E water and 500/1000 TIP4P water are displayed in Fig. 6. The plane of basal oxygen atoms of the tetrahedral surface is taken as a reference distance ($z = 0$ Å) and a vertical solid line in Fig. 6 schematically represents the plane of oxygen atoms from the surface hydroxyl groups. The shape of curves is simple having one relatively narrow peak confirming the formation of the monomolecular water layer as visually observed in Fig. 2. The maxima of all peaks are in a narrow interval of ~0.3 Å with a perpendicular distance to the plane of hydroxyl oxygen atoms of about 2.6–2.9 Å. This finding is in a very good agreement with the distance of ~2.7 Å computed in the periodic DFT study of the monomolecular water layer on the octahedral surface (Tunega et al., 2004). The difference between the SPC/E and TIP4P results is small; the maxima of the TIP4P curves are only a slightly shifted to the lower values.

3.2.2. Tetrahedral surface

Fig. 3a shows front view of the initial configuration of the water nanodroplet containing 500 SPC/E water molecules on the (001) tetrahedral surface of the kaolinite layer. Fig. 3b and c represent front and top side views of a snapshot collected after 5 ns. It is evident that the water droplet behaves completely differently comparing to the octahedral surface (Fig. 2). The water molecules stay together as a compact entity keeping a form of deformed sphere. It means that interactions of water molecules with the tetrahedral surface are weaker than interactions within the water droplet. Since the contact between the droplet and the surface is relatively weak, a slow lateral movement of the whole droplet on the surface has been observed. Moreover, several water molecules spontaneously evaporated from the droplet into vacuum. After a certain time, some of evaporated molecules returned back to the droplet and the rest flew through the whole vacuum and landed on the opposite octahedral surface (see Fig. 3).

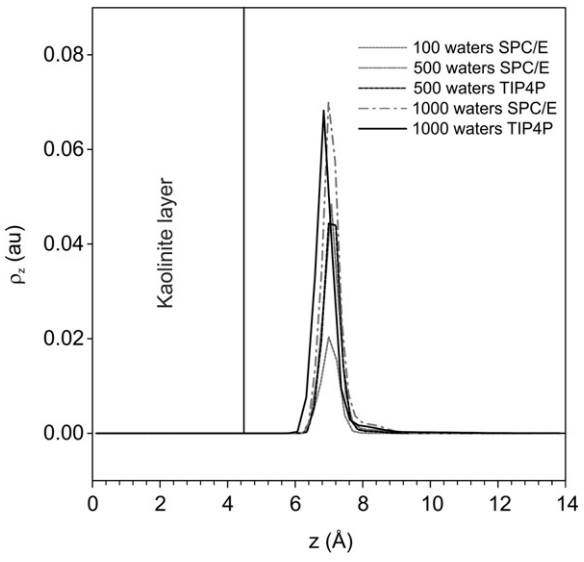

Fig. 6. Atomic z-density profiles ρ_z (in arbitrary units) of water oxygen atoms for last 2 ns of MD simulation for the (001) octahedral surface of kaolinite layer and water droplets with $N_w = 100$ (SPC/E) and $N_w = 500/1000$ (SPC/E and TIP4P). Vertical solid line represents plane of oxygen atoms of the surface OH groups, $z = 0$ represents plane of basal oxygen atoms of the tetrahedral surface.

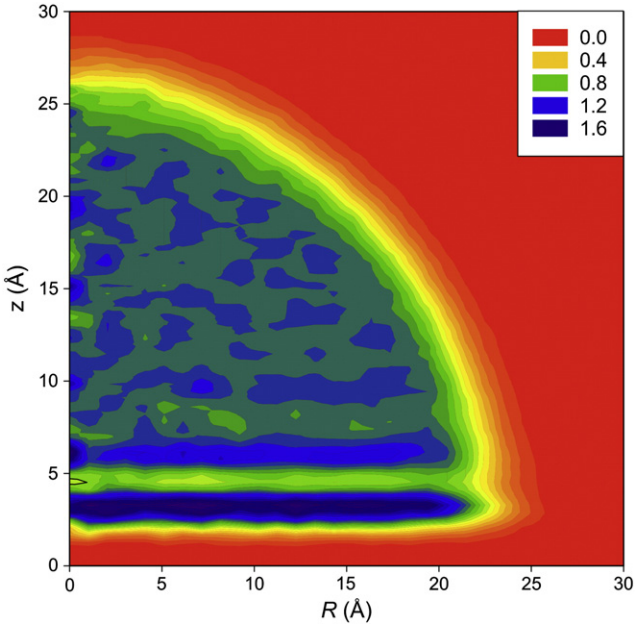

Fig. 7. Visualization of water density profile (in g/cm^3) of water droplet ($N_w = 1000$, TIP4P) on the (001) tetrahedral kaolinite surface calculated for last 2 ns of MD simulation.

The method of cylindrical bins was used for analysis of the shape of the water droplet on the tetrahedral surface. Fig. 7 presents a color visualization of time-averaged water density field (in g/cm^3) of the water droplet model ($N_w = 1000$, TIP4P). The water density fields of other water models with 500 and 1000 molecules are similar and are not presented. Fig. 7 shows very clearly a shape of the water droplet on the kaolinite tetrahedral surface ($z = 0$ in Fig. 7). The boundary between liquid and gas phase is well distinguished (yellow color in Fig. 7). The water density in the droplet is not homogeneous, especially near the tetrahedral surface. In the vicinity of the surface a formation of water layer with thickness of 1.0–1.2 Å is observed at a distance of 2.5–3.0 Å to the surface. The thickness of this layer indicates that the layer is monomolecular. It has a relatively homogeneous lateral density that is higher than a normal water bulk density. This layer is followed by a water layer with lower density separating the first layer and the rest of the droplet. In Fig. 7 the third relatively homogeneous water layer is still quite well distinguished. Observed water layer separation near the kaolinite surface is also well documented by plotted one-dimensional atomic density profiles along the z-axis as shown in Fig. 8 where curves for all studied models of the tetrahedral surface are shown. The clear maxima and minima on curves are observed what corresponds to the formation of water layers with a varying density in a vicinity of the surface as described above. Some additional minima and maxima are still distinguishable at larger distances from the surface ($z > \sim 8$ Å). A similar shape of one-dimensional z-densities was obtained in a study of water droplet on a graphite surface (Lundgren et al., 2002). The water layering shows that in spite of relatively weak interactions between the tetrahedral surface and the water droplet, the surface has a polarization effect on the droplet and water molecules in the vicinity of the surface have a preferred orientation. Similar water layer separation near surface was also observed in the contact angle simulation of water droplets on LJ surfaces with varying LJ parameters (Hong et al., 2009). The SPC, SPC/E, and TIP4P water models give similar results as can be seen in Fig. 8. Only the maxima of TIP4P water models are slightly shifted to higher values in comparison to two other water models.

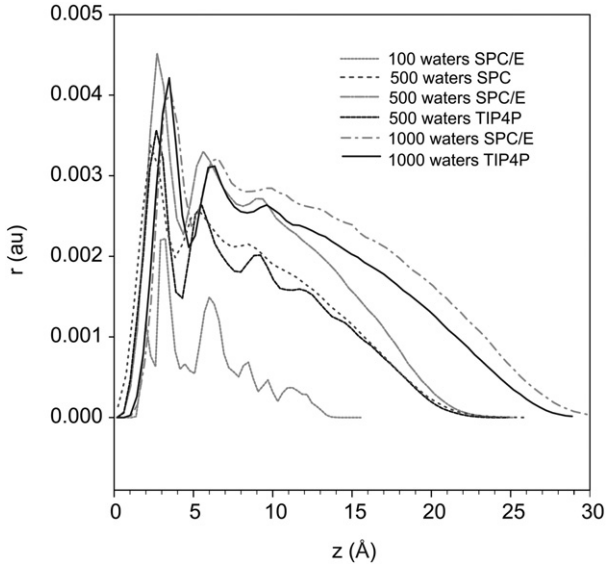

Fig. 8. Atomic *z*-density profiles ρ_z (in arbitrary units) of water oxygen atoms for last 2 ns of MD simulation for all models of the water droplet on the (001) tetrahedral surface of the kaolinite layer.

The water layer separation and water density fluctuation close to the kaolinite surface represented a certain complication in finding points on liquid–gas interface (Eq. (3)), thus first several *z*-slabs near the surface were not taken into an account in a fitting procedure. Radii R_B of five fitted circles are presented in Table 4 together with corresponding computed contact angles. Comparing R_B radii certain differences among the water models are observed. This is more evident for the smaller droplet (500 molecules). In spite of that fact, all water models give almost identical values of the contact angle with no difference between the droplets with 500 and 1000 molecules, respectively (Table 4). The computed CA value is of 104° for the SPC and SPC/E water models, and of 106° for the TIP4P, respectively. According basic characterization of wettability of solid surfaces on the base of the water contact angle, the tetrahedral (001) kaolinite surface can be considered as hydrophobic what corresponds to a previous characterization in theoretical DFT studies (e.g. Tunega et al., 2004).

The experimentally determined values of the contact angle for kaolinite were in a range of 17–20° (Shang et al., 2010) depending on the relative humidity. It seems to be a large disagreement between theoretically calculated and experimentally measured contact angle. We suppose that this disagreement is only apparent and has a plausible explanation. There are several important differences between experiment and simulation. In the experiment (sessile drop method), a macroscopic droplet (several μL) was measured on a clay film prepared from a clay suspension containing clay particles with a size <2 μm. Thin clay film was prepared by drying of the clay suspension placed on a glass slide. Thus, in such case a macroscopic clay surface is formed as a superposition of microscopic surfaces of mineral particles preferentially oriented on the glass slide. Probably both types of the (001) basal surfaces will dominate in such clay films due to a typical shape of kaolinite particles (thin flakes) and a preferential orientation on the glass slide. Formed macroscopic surface of kaolinite is very porous and rough, where probably hydrophobic and hydrophilic domains alter. This all contributes to overall average wettability of measured surface. Moreover, it is very difficult to estimate a ratio among different surfaces. The complex character of the real kaolinite surface has the main impact on the final shape of the macroscopic water droplet and corresponding measured value of the contact angle. In opposite, our simulations are performed separately for two ideal surfaces using water nanodroplets, much smaller than experimental microdroplets. However, it seems that the size of the nanodroplet in simulations is not a critical factor. It has been shown in the simulations of LJ liquids and droplets on a planar surface that an extrapolation of the size of the droplet to an "infinite" dimension changes contact angle only in a range of few degrees (Ingebrigtsen and Toxvaerd, 2007). Our theoretically estimated values (0° for octahedral and ~105° for tetrahedral surface) can be considered as boundary values and if a real kaolinite surface is a mixture mainly of these two surface types a real value of macroscopic contact angle should lay in that interval.

Table 4
Computed radius of fitted circle (R_B) and corresponding contact angle (θ) for the tetrahedral kaolinite surface obtained with SPC, SPC/E, and TIP4P water droplets having 500/1000 molecules.

	R_B (Å)	θ (°)
500 SPC water droplet	14.22	104
500 SPC/E water droplet	17.61	104
500 TIP4P water droplet	19.42	106
1000 SPC/E water droplet	23.12	104
1000 TIP4P water droplet	24.11	106

4. Conclusions

Wettability of two ideal surfaces (tetrahedral and octahedral) of the kaolinite layer parallel to the (001) basal plane has been investigated by means of force-field molecular dynamics simulations of interactions of water nanodroplets. The simulations showed that the octahedral surface formed from surface hydroxyl groups is fully hydrophilic. In the simulations on the octahedral surface the water droplets were spread over the surface forming incomplete network of monomolecular water layer. This network is bound to the surface via multiple hydrogen bonds where the surface hydroxyl groups act as a proton donor and/or acceptor, respectively. The incomplete water network is structured reflecting a quasi-hexagonal arrangement of surface hydroxyl groups.

In case of the tetrahedral surface water molecules stayed together keeping the deformed shape of the droplet. Although the interactions of water molecules with the basal oxygen atoms are in the form of hydrogen bonds, they are much weaker than in case of the octahedral surface. Moreover, the hydrogen bonds inside of the droplet are stronger than those with the tetrahedral surface. The analysis of the water density of the droplets showed that in spite of the weak interactions with the surface, several structured and ordered monomolecular water layers are formed in the droplet in the vicinity of the surface as a consequence of the polarization effect of the surface. The computed microscopic contact angle is about 105° what demonstrates that the tetrahedral kaolinite surface is hydrophobic. The computed contact angle was well reproduced with two different sizes of water nanodroplets (500 and 1000 molecules) and with three different water models (SPC, SPC/E, and TIP4P). The experimental values of the contact angle for kaolinite indicate that the overall character of the kaolinite surface is hydrophilic and our calculations have shown that surface hydroxyl groups are responsible for that.

Acknowledgments

The authors are grateful for the financial support from the Austrian Science Fund, project no. P20893-N19, and the German Research Foundation, the priority program SPP 1315, project no. GE1676/1-1. We also acknowledge the technical support and computer time at the Vienna Scientific Cluster.

References

Adams, J.M., 1983. Hydrogen-atom positions in kaolinite by neutron profile refinement. Clays and Clay Minerals 31 (5), 352–356.
Bailey, S.W., 1988. Hydrous phyllosilicates — introduction. Reviews in Mineralogy 19, 1–8.

Berendsen, H.J.C., Grigera, J.R., Straatsma, T.P., 1987. The missing term in effective pair potentials. Journal of Physical Chemistry 91 (24), 6269–6271.
Berendsen, H.J.C., Postma, J.P.M., van Gunsteren, W.F., Hermans, J., 1981. In: Pullman, B. (Ed.), Intermolecular Forces. Reidel, Dordrecht, p. 331.
Bish, D.L., 1993. Rietveld refinement of the kaolinite structure at 1.5-k. Clays and Clay Minerals 41 (6), 738–744.
Croteau, T., Bertram, A.K., Patey, G.N., 2008. Adsorption and structure of water on kaolinite surfaces: possible insight into lee nucleation from grand canonical Monte Carlo calculations. Journal of Physical Chemistry A 112 (43), 10708–10712.
Croteau, T., Bertram, A.K., Patey, G.N., 2009. Simulation of water adsorption on kaolinite under atmospheric conditions. Journal of Physical Chemistry A 113 (27), 7826–7833.
Cruz-Chu, E.R., Aksimentiev, A., Schulten, K., 2006. Water-silica force field for simulating nanodevices. Journal of Physical Chemistry B 110 (43), 21497–21508.
Cygan, R.T., Liang, J.J., Kalinichev, A.G., 2004. Molecular models of hydroxide, oxyhydroxide, and clay phases and the development of a general force field. Journal of Physical Chemistry B 108 (4), 1255–1266.
de Ruijter, M.J., Blake, T.D., De Coninck, J., 1999. Dynamic wetting studied by molecular modeling simulations of droplet spreading. Langmuir 15 (22), 7836–7847.
Ewald, P.P., 1921. The calculation of optical and electrostatic grid potential. Annalen Der Physik 64 (3), 253–287.
Giovambattista, N., Debenedetti, P.G., Rossky, P.J., 2007. Effect of surface polarity on water contact angle and interfacial hydration structure. Journal of Physical Chemistry B 111 (32), 9581–9587.
Helmy, A.K., Ferreiro, E.A., de Bussetti, S.G., 2004. The surface energy of kaolinite. Colloid and Polymer Science 283 (2), 225–228.
Hockney, R.W., Eastwood, J.W., 1988. Computer Simulation using Particles. Taylor & Francis Group, New York.
Hong, S.D., Ha, M.Y., Balachandar, S., 2009. Static and dynamic contact angles of water droplet on a solid surface using molecular dynamics simulation. Journal of Colloid and Interface Science 339 (1), 187–195.
Hu, X.L., Michaelides, A., 2007. Ice formation on kaolinite: lattice match or amphoterism? Surface Science 601 (23), 5378–5381.
Hu, X.L., Michaelides, A., 2008. Water on the hydroxylated (001) surface of kaolinite: from monomer adsorption to a flat 2D wetting layer. Surface Science 602 (4), 960–974.
Ingebrigtsen, T., Toxvaerd, S., 2007. Contact angles of Lennard-Jones liquids and droplets on planar surfaces. Journal of Physical Chemistry C 111 (24), 8518–8523.
Jorgensen, W.L., Madura, J.D., 1985. Temperature and size dependence for monte-carlo simulations of tip4p water. Molecular Physics 56 (6), 1381–1392.
Kusalik, P.G., Svishchev, I.M., 1994. The spatial structure in liquid water. Science 265 (5176), 1219–1221.
Lundgren, M., Allan, N.L., Cosgrove, T., 2002. Wetting of water and water/ethanol droplets on a non-polar surface: a molecular dynamics study. Langmuir 18 (26), 10462–10466.
Neder, R.B., et al., 1999. Refinement of the kaolinite structure from single-crystal synchrotron data. Clays and Clay Minerals 47 (4), 487–494.
Ohler, B., Langel, W., 2009. Molecular dynamics simulations on the interface between titanium dioxide and water droplets: a new model for the contact angle. Journal of Physical Chemistry C 113 (23), 10189–10197.
Park, J.H., Aluru, N.R., 2009. Temperature-dependent wettability on a titanium dioxide surface. Molecular Simulation 35 (1–2), 31–37.
Plimpton, S., 1995. Fast parallel algorithms for short-range molecular-dynamics. Journal of Computational Physics 117 (1), 1–19.
Rae, J., Parker, A., 1988. Environmental Interactions of Clays. Springer Verlag, Berlin.
Ryckaert, J.P., Ciccotti, G., Berendsen, H.J.C., 1977. Numerical-integration of Cartesian equations of motion of a system with constraints — molecular-dynamics of n-alkanes. Journal of Computational Physics 23 (3), 327–341.
Schachtschabel, P., Blume, H.P., Brümmer, G., Hartge, K.-H., Schwertmann, U., 1989. Lehrbuch der Bodenkunde. Ferdinant Enke Verlag, Stuttgart.
Shang, J.Y., Flury, M., Harsh, J.B., Zollars, R.L., 2010. Contact angles of aluminosilicate clays as affected by relative humidity and exchangeable cations. Colloids and Surfaces a-Physicochemical and Engineering Aspects 353 (1), 1–9.
Shi, B., Dhir, V.K., 2009. Molecular dynamics simulation of the contact angle of liquids on solid surfaces. Journal of Chemical Physics 130 (3).
Smirnov, K.S., Bougeard, D., 1999. A molecular dynamics study of structure and short-time dynamics of water in kaolinite. Journal of Physical Chemistry B 103 (25), 5266–5273.
Swope, W.C., Andersen, H.C., Berens, P.H., Wilson, K.R., 1982. A computer-simulation method for the calculation of equilibrium-constants for the formation of physical clusters of molecules — application to small water clusters. Journal of Chemical Physics 76 (1), 637–649.
Tunega, D., Benco, L., Haberhauer, G., Gerzabek, M.H., Lischka, H., 2002a. Ab initio molecular dynamics study of adsorption sites on the (001) surfaces of 1: 1 dioctahedral clay minerals. Journal of Physical Chemistry B 106 (44), 11515–11525.
Tunega, D., Gerzabek, M.H., Lischka, H., 2004. Ab initio molecular dynamics study of a monomolecular water layer on octahedral and tetrahedral kaolinite surfaces. Journal of Physical Chemistry B 108 (19), 5930–5936.
Tunega, D., Haberhauer, G., Gerzabek, M.H., Lischka, H., 2002b. Theoretical study of adsorption sites on the (001) surfaces of 1: 1 clay minerals. Langmuir 18 (1), 139–147.
Vaz, C.M.P., Herrmann, P.S.P., Crestana, S., 2002. Thickness and size distribution of clay-sized soil particles measured through atomic force microscopy. Powder Technology 126 (1), 51–58.
Warne, M.R., Allan, N.L., Cosgrove, T., 2000. Computer simulation of water molecules at kaolinite and silica surfaces. Physical Chemistry Chemical Physics 2 (16), 3663–3668.
Werder, T., Walther, J.H., Jaffe, R.L., Halicioglu, T., Koumoutsakos, P., 2003. On the water-carbon interaction for use in molecular dynamics simulations of graphite and carbon nanotubes. Journal of Physical Chemistry B 107 (6), 1345–1352.
Young, R.A., Hewat, A.W., 1988. Verification of the triclinic crystal-structure of kaolinite. Clays and Clay Minerals 36 (3), 225–232.